PVP-Vol. 225 / NE-Vol. 7

RECENT ADVANCES IN STRUCTURAL MECHANICS

– 1991 –

EDITED BY
H. H. CHUNG
Y. W. KWON

PVP-Vol. 225 / NE-Vol. 7

RECENT ADVANCES IN STRUCTURAL MECHANICS
– 1991 –

presented at
THE WINTER ANNUAL MEETING OF
THE AMERICAN SOCIETY OF MECHANICAL ENGINEERS
ATLANTA, GEORGIA
DECEMBER 1-6, 1991

sponsored by
THE PRESSURE VESSELS AND PIPING DIVISION, ASME
THE NUCLEAR ENGINEERING DIVISION, ASME

edited by
HOWARD H. CHUNG
ARGONNE NATIONAL LABORATORY

YOUNG W. KWON
NAVAL POSTGRADUATE SCHOOL

THE AMERICAN SOCIETY OF MECHANICAL ENGINEERS
345 East 47th Street ○ ○ United Engineering Center ○ ○ New York, N.Y. 10017

ISBN No. 0-7918-0899-8

Library of Congress
Catalog Number 91-58606

FOREWORD

This publication contains nineteen papers presented at the symposium entitled "Recent Advances in Structural Mechanics" at the 1991 ASME Winter Annual Meeting held in Atlanta, Georgia. The symposium was sponsored by the Operations, Applications, and Components Committee of the Pressure Vessels and Piping Division.

This publication consists of four parts:

- Structural Instability
- Fracture and Fatigue in Composites
- Pressure Vessels and Piping
- Design and Analysis

Five papers on structural instability discussed pre- and post-buckling problems with static and dynamics loads. The second part has five papers dealing with fracture and fatigue problems occurring in composite structures. Four articles in the next part discuss recent technology in pressure vessels and piping. Finally, the last part has five papers devoted to the enhancement of design and analysis methods in structural mechanics, especially in composite structures.

The work reported here is representative of current research activities and contributes to the advancement of structural mechanics. The editors hope that this volume will serve as a useful resource for structural engineers and stimulate further interest in structural mechanics research.

The editors wish to express their sincere gratitude to the authors for their contributions to the symposium and to the reviewers for their critical comments and conscientious criticism.

Howard H. Chung
Argonne National Laboratory
Argonne, Illinois

Young W. Kwon
Naval Postgraduate School
Monterey, California

CONTENTS

DESIGN AND ANALYSIS

PVP-Vol. 225/NE-Vol. 7, Recent Advances in
Structural Mechanics
ASME 1991

FREQUENCY-COMPRESSIVE LOAD INTERACTIONS IN THE PRE-AND POSTBUCKLING RANGES OF GEOMETRICALLY IMPERFECT DOUBLY CURVED COMPOSITE SHALLOW SHELLS

Liviu Librescu
Department of Engineering Science and Mechanics
Virginia Polytechnic Institute and State University
Blacksburg, Virginia

M. Y. Chang
Department of Mechanical Engineering
National Chung-Hsing University
Taichung, Taiwan, Republic of China

ABSTRACT

Laminated composite structures are being increasingly used in the aeronautical and aerospace constructions. Employment of the new composite material systems exhibiting exotic properties such as high degrees of anisotropy and low rigidities in transverse shear require more accurate methods of analysis which are obtained by discarding the classical Kirchhoff assumptions.

The purpose of the present paper is to determine the vibrational behavior of preloaded geometrically imperfect laminated composite curved panels. Such an item is of an essential importance in the analysis of the flutter instability, forced vibration and dynamic response of structures.

As a preparatory step, a refined geometrically non–linear theory of transversely–isotropic symmetrically laminated composite panels, extended to include the dynamic effects is developed. The theory developed within the Lagrange description is based on a higher–order representation of the in–plane displacement field through the thickness of the structure and incorporates the effects of transverse shear deformation, transverse normal stress component, the out–of–plane initial geometric imperfection and fulfills that static conditions on the bounding surfaces of the shell. The governing non–linear equations are reduced, by using a single arbitrary mode approach in conjunction with Galerkin's method, to a single non–linear ordinary differential equation.

The numerical results allow one to obtain a series of conclusions concerning the influence played by the stress–free initial imperfections; transverse shear deformation; the character of in–plane boundary conditions and the non–homogeneity of the structure, on vibration frequencies of in–plane loaded composite panels in the pre– and postbuckling ranges.

INTRODUCTION

The study of the free vibration of homogeneous and composite flat and curved panels has been the subject of a considerable interest over the past ten years. However, very few analyses have been devoted to the study of the effects played by the small, usually unavoidable geometric imperfections on the vibration frequencies of composite shear–deformable curved panels subjected to conservative in–plane preloads. Initial geometric imperfections have been found to be very significant in affecting the small–amplitude vibration frequencies of flat and curved panels subjected to in–plane compressive preloads. On the other hand, the new exotic composite material systems exhibit low rigidities in transverse shear and as a result, the theory of structures made of such materials should be based on a refined model obtained by discarding the Love–Kirchhoff hypothesis.

The present paper is going to analyze the effects of initial geometric imperfections and transverse shear deformations on the vibration frequency of uni/biaxially compressed shear deformable laminated composite curved panels. In addition to the influence of the above mentioned effects, the one played by the sign of the Gaussian curvature of the mid–surface of the curved panel will also be investigated. However, in order to be able to study this problem, as a preparatory step, the governing equations of shear deformable composite curved panels should be derived. It should be remarked that in spite of its evident importance very few papers have incorporated the effect of transverse shear flexibility in the study of this problem. In the majority of cases this problem was analyzed for flat panels (Bhimaraddi, 1989a, b) or within the Love–Kirchhoff model (Hui and Leissa, 1983; Hui, 1985; Ilanko and Dickinson, 1987; Singer and Prucz, 1982; and Elishakoff et al., 1987).

GEOMETRICALLY NON–LINEAR THEORY OF SHEAR DEFORMABLE LAMINATED COMPOSITE CURVED PANELS

Consider the case of laminated composite doubly–curved shallow panels of uniform thickness h, symmetrically laminated of 2m+1 (m=1,2...) elastic transversely–isotropic layers. It is assumed that the planes of isotropy of the layer materials are parallel at each point to the reference surface σ of the composite panel. By adopting the assumption proper to the shallow shell theory, by considering a higher–order representation for the in–plane displacement field

through the shell thickness (see e.g. Librescu and Stein, 1991), by retaining in the geometrical equations the nonlinear terms associated with the transversal displacement component only, we obtain within the Lagrange description a system of three partial differential governing equations. Expressed in a tensorial form these equations are:

$$
\begin{aligned}
&Du_3\Big|^{\alpha\beta}_{\alpha\beta} - c^{\alpha\omega}\, c^{\beta\rho}\Big\{b_{\alpha\beta}\, F_{|\,\omega\rho} + \Big[u_{3|\,\alpha\beta} + \overset{o}{u}_{3|\,\alpha\beta}\Big]\, F_{|\,\omega\rho} \\
&\quad - \Big[\frac{B+C}{S} - \delta_A \frac{M}{S}\Big]\Big[b_{\alpha\beta}\, F_{|\,\omega\rho} + F_{|\,\omega\rho}\Big[u_{3|\,\alpha\beta} \\
&\quad - \Big[p_3 - \Big[\frac{B+C}{S} - \delta_A \frac{M}{S}\Big] p_3\Big|^{\sigma}_{\sigma}\Big] \qquad (1)_1 \\
&\quad + m_o\Big[\ddot{u}_3 - \Big[\frac{B+C}{S} + \delta_A \delta_C\Big[\frac{F}{m_o} - \frac{M}{S}\Big]\Big]\, \ddot{u}_3\Big|^{\alpha}_{\alpha}\Big] = 0\,,
\end{aligned}
$$

$$
\begin{aligned}
&(\tilde{b}+\tilde{c})\, F\Big|^{\lambda\pi}_{\lambda\pi} + \frac{1}{2}\Big[u_3\Big|^{\rho}_{\rho} u_3\Big|^{\lambda}_{\lambda} - u_3\Big|^{\lambda}_{\rho} u_3\Big|^{\rho}_{\lambda}\Big] \\
&\quad + \Big[\overset{o}{u}_3\Big|^{\pi}_{\pi} u_3\Big|^{\alpha}_{\alpha} - \overset{o}{u}_3\Big|^{\pi}_{\alpha} u_3\Big|^{\alpha}_{\pi}\Big] + \Big[2H u_3\Big|^{\pi}_{\pi} - b^{\beta}_{\lambda} u_3\Big|^{\lambda}_{\beta}\Big] \qquad (1)_2 \\
&\quad + 2\delta_A \tilde{d}\Big[u_3\Big|^{\lambda\rho}_{\lambda} u_3\Big|_{\rho} + u_3\Big|^{\lambda}_{\rho} u_3\Big|^{\rho}_{\lambda} + \overset{o}{u}_3\Big|^{\rho\pi}_{\pi} u_3\Big|_{\rho} \\
&\quad + u_3\Big|^{\rho\pi}_{\pi} \overset{o}{u}_3\Big|_{\rho} + + 2\overset{o}{u}_3\Big|^{\rho}_{\pi} u_3\Big|^{\pi}_{\rho}\Big] = 0
\end{aligned}
$$

and

$$
\phi - \frac{C}{S}\,\phi\Big|^{\sigma}_{\sigma} = 0. \qquad (1)_3
$$

These equations (which are not going to be derived here) represent the generalized counterpart of von Kármán large deflection plate theory (derived within the classical Kirchhoff hypothesis) as well as of the Reissner's plate theory generalized for the theory of shells (see e.g. Librescu, 1975).

In these equations $u_3 (\equiv u_3(x_\alpha, t))$, $F (\equiv F(x_\alpha, t))$ and $\psi (\equiv \psi(x_\alpha, t))$ denote the transverse deflection, Airy potential function and a transverse shear potential function, respectively; $\overset{o}{u}_3 (\equiv \overset{o}{u}_3(x_\alpha))$ denotes the initial out–of–plane geometric imperfection, while D, B, C, F, S, M denote the rigidity quantities (not displayed in the paper); δ_A and δ_H are tracing quantities which take the values zero or one according to whether the influence identified by them (i.e., of the transverse normal stress and of higher order effects) is disregarded or taken into account, respectively while the dots denote time derivatives. In addition $(\cdot)|^{\alpha}_{\alpha}$ and $(\cdot)|^{\alpha\beta}_{\alpha\beta}$ denote the Laplace and biharmonic operators, respectively. $(\,)|_{\alpha}$ denotes the covariant derivative with respect to the in–plane coordinates x_α of the mid–surface of the shell; b^{α}_{β} denotes the curvature tensor of the undeformed mid–surface of the shell while $c^{\alpha\beta}$ denotes the 2–D permutation symbol.

Having in view that within the geometrically nonlinear theory of plates and shells, the bending state of stress is coupled with the stretching one, both out–of–plane and in–plane boundary conditions are involved.

In the following developments, the case of simply supported boundary conditions on the whole contour will be considered. While the out–of–plane boundary conditions are exactly fulfilled, the in–plane ones are fulfilled **on an average**. The details of these developments are not displayed here. Employment of the procedure developed in Librescu and Stein, 1991 and Librescu, 1975 allows one to obtain the equation describing the interaction between the frequency and the compressive edge loads in the pre– and postbuckling ranges. This equation which is very intricate will not be displayed here.

NUMERICAL ILLUSTRATIONS AND CONCLUSIONS

The numerical illustrations concern the cases of single and three layered composite shallow curved panels. As concern the **composite** curved panel two instances labelled as Case 1 and Case 2 are considered, i.e.,

Case 1

$$
\frac{E_{<2>}}{G'_{<2>}} = 10;\ \frac{E_{<1>}}{G'_{<1>}} \left(\equiv \frac{E_{<3>}}{G'_{<3>}}\right) = 30;\ \frac{E_{<1>}}{E'_{<1>}} \left(\equiv \frac{E_{<3>}}{E'_{<3>}} = 5\right.
$$

$$
\frac{E_{<2>}}{E'_{<2>}} = 2;\ \frac{E_{<1>}}{E'_{<2>}} \left(\equiv \frac{E_{<3>}}{E'_{<3>}} = 10.\right.
$$

Case 2

$$
\frac{E_{<2>}}{G'_{<2>}} = 30;\ \frac{E_{<1>}}{G'_{<1>}} \left(\equiv \frac{E_{<3>}}{G'_{<3>}}\right) = 10;\ \frac{E_{<1>}}{E'_{<1>}} \left(\equiv \frac{E_{<3>}}{E'_{<3>}} = 5\right.
$$

$$
\frac{E_{<2>}}{E'_{<2>}} = 2;\ \frac{E_{<1>}}{E_{<2>}} \left(\equiv \frac{E_{<3>}}{E_{<2>}} = 10.\right.
$$

For both cases the Poisson's ratios are

$$
\nu'_{<r>} = \nu_{<r>} = \nu'_{<m+1>} = \nu_{<m+1>} = 0.25.
$$

It is assumed that the mid–layer of the three–layered plate is two times thicker than the external ones (implying that $h_{<1>}/h \,(\equiv h_{<3>}/h) = 0.5$ and $h_{<2>}/h = 0.25$).

Here E, ν and E′, ν' denote the Young's modulus and Poisson's ratio in the planes of isotropy and in the planes transverse to the isotropy planes, respectively, while G′ denotes the transverse shear modulus.

In Fig. 1 the effect of the ratio E/G′ (which constitutes a measure of the transverse shear flexibility) on the normalized eigenfrequency of a circular cylindrical panel (perfect and

imperfect) subjected to the (normalized) uniaxial edge loads $\tilde{L}_1^*$ is displayed. The results reveal that in the prebuckling range the Love–Kirchhoff shell model yields higher eigenfrequencies than the ones provided by the refined theory. However in the postbuckling range the opposite trend holds valid. In other words, the classical theory of shells overpredicts the eigenfrequencies in the prebuckling range and underpredicts them in the postbuckling range. This trend whose explanation will be given at the Conference holds valid for both perfect and imperfect shells.

It should be noted that the negative portions of the frequency curves correspond to an unstable postbuckling path. This means that with the increase or decrease of the compressive edge load some jumps in the eigenfrequencies are expected to occur. Figure 2 displays the variation of the nondimensional eigenfrequency $\tilde{\omega}^2 \left(\equiv -\frac{m_o}{D}\left(\frac{\ell_1}{\pi}\right)^4 \omega^2\right)$ vs. the nondimensional uniaxial load $\tilde{L}_1 \left(\equiv \frac{L_{11}\ell_1^2}{\pi^2 D}\right)$ for circular cylindrical panels of various ratios ℓ_2/R_2. The figure reveals that with the increase of the ratios ℓ_2/R_2 higher eigenfrequencies are obtained both within the CLT (classical theory) and HSDT (higher order shear deformation theory). As concerns the eigenfrequencies as predicted by CLT and HSDT in the pre– and postbuckling ranges, their trend mentioned before is also repeated within this figure.

Figure 3 compares the eigenfrequencies of uniaxial compressed circular cylindrical panels for movable and immovable edge conditions. The result displayed here for a perfect panel reveal that for immovable edge panels, in contrast to their movable counterparts, the eigenfrequencies do not exhibit unstable paths. In addition, they exhibit a continuous increase which is associated with the increase of compressive (uniaxial) edge loads. However, the eigenfrequencies associated with the movable edge panels exhibit in the postbuckling range a stronger increase as compared to their immovable panel counterpart. The same figure also reveals that for single layered panels the HSDT provides results in excellent agreement with FSDT when the shear correction factor is selected as $K^2 = 5/6$.

Figure 4 compares the nondimensional eigenfrequencies $\tilde{\omega}^2$ for uniaxially compressed doubly curved panels in the pre– and postbuckling ranges and within CLT and HSDT. The results reveal that for positive Gaussian curvature shells, in contrast to their negative or zero Gaussian curvature counterparts, the classical theory overestimates the frequencies over a larger range of compressive loads. Moreover, for negative Gaussian curvature shells, the increase of the negative curvature is accompanied by a diminution of the compressive loads at which the trend played by CLT (consisting of the overprediction of the eigenfrequencies) is reversed.

Figure 5 presents the influence of positive (downward) and negative (upward) out–of–plane imperfections on the eigenfrequencies of shells with negative Gaussian curvature compressed by uniaxial edge loads. The results reveal that for low compressive loads, the shells with negative imperfections result in higher eigenfrequencies than their counterparts with positive imperfections. However, for higher ranges of uniaxial edge compressive loads, this trend is reversed.

Figure 6 displays the variation of $\tilde{\omega}^2$ vs. $\tilde{L}_1$ for the three–layered composite circular cylindrical panels compressed by uniaxial edge loads. Two cases, i.e., Case 1 and Case 2 of the three–layered composite structure are considered. The results reveal that the increase of the transverse shear flexibility (TSF) of the face layers (Case 1) yields a stronger increase of the eigenfrequencies in the postbuckling range, as compared to the case when the increase of TSF occurs in the core layer only (Case 2). It is also revealed that the classical theory, postulating invariably that $E/G' = 0$, predicts the same results for both cases, i.e., the lowest frequencies in the postbuckling range and the highest frequencies in the pre–buckling one.

In addition, the results reveal that in contrast to the single layered case, the FSDT with $K^2 = 2/3$ provides results in better agreement with HSDT than the FSDT with $K^2 = 5/6$. Other conclusions related to the vibratory behavior of imperfect shells will be presented at the Conference.

REFERENCES

Bhimaraddi, A., 1989, "Non–Linear Free Vibration Analysis of Composite Plates with Initial Imperfections and In–Plane Loadings," Int. J. Solids Structures, Vol. 25, No. 1, pp. 33–43.

Bhimarraddi, A., 1989, "Nonlinear Vibrations of In–Plane Loaded Imperfect, Orthotropic Plates Using the Perturbation Technique," Int. J. Solids Structures, Vol. 25, No. 5, pp. 563–575.

Elishakoff, I., Birman, V. and Singer, J., 1987, "Small Vibrations on an Imperfect Panel in the Vicinity of a Nonlinear Static Case," J. Sound Vibration, 114, pp. 57–63.

Hui, D. and Leissa, A. W., 1983, "Effects of Geometric Imperfections on Vibrations of Biaxially Compressed Rectangular Flat Plates," J. Appl. Mech., 50, pp. 750–756.

Hui, D., 1985, "Effects of Geometric Imperfections on Frequency–Load Interaction of Biaxially Compressed Anti–symmetric Angle Ply Rectangular Plates," J. Appl. Mech., 52, pp. 155–161.

Ilanko, S. and Dickinson, S. M., 1987, "The Vibration and Post–Buckling of Geometrically Imperfect Simply Supported, Rectangular Plates Under Uni–Axial Loading; Part I, Theoretical Approach," J. Sound Vibration, 118, pp. 313–336.

Librescu, L. and Stein, M., 1991, "A Geometrically Nonlinear Theory of Shear Deformable Laminated Composite Plates and Its Use in the Postbuckling Analysis," Proceedings of the International Congress of the Aeronautical Science, Vol. 1, Jerusalem, Israel, August 28 – September 2, 1988, pp. 349–359 (an amended version of this paper was published in "Thin Walled Structures – Special Aerospace Structures Issue, 11, 1991, pp. 177–201).

Librescu, L., 1975, Elastostatics and Kinetics of Anisotropic and Heterogeneous Shell–Type Structures, Noordhoff International Publishing, Leyden, The Netherlands.

Singer, J. and Prucz, J., 1982, "Influence on Initial Geometrical Imperfections on Vibrations of Axially Compressed Stiffened Cylindrical Shells," J. of Sound and Vibration, 80, 1, pp. 117–143.

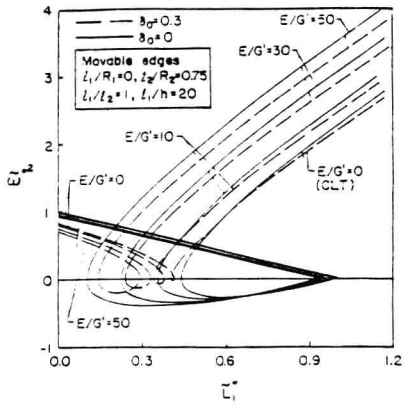

Figure 1. Frequency–Load Interaction in the Pre– and Postbuckling Ranges

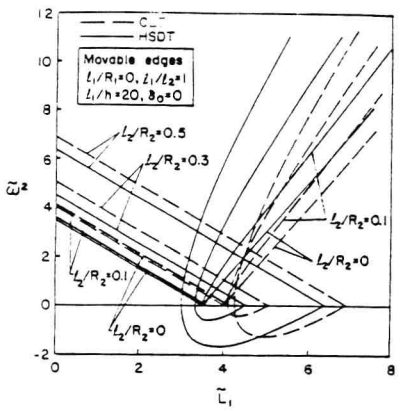

Figure 2. Frequency–Load Interaction in the Pre– and Postbuckling Ranges

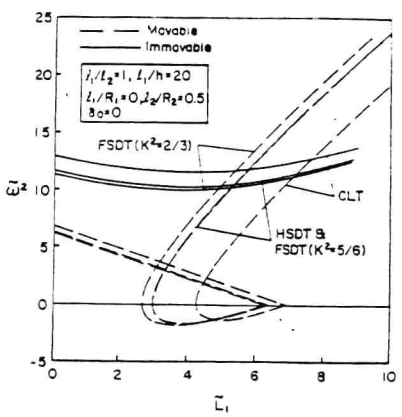

Figure 3. Frequency–Load Interaction in the Pre– and Postbuckling Ranges

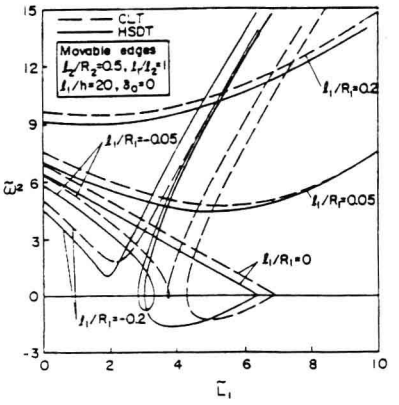

Figure 4. Frequency–Load Interaction in the Pre– and Postbuckling Ranges

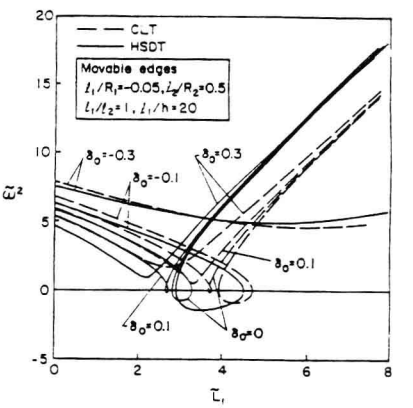

Figure 5. Frequency–Load Interaction in the Pre– and Postbuckling Ranges

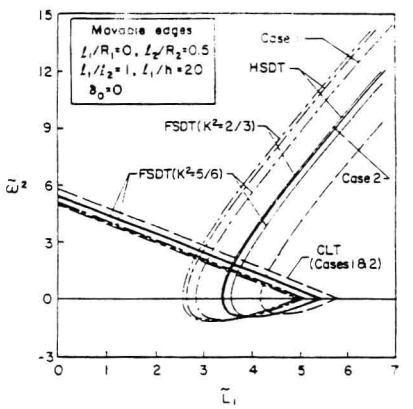

Figure 6. Frequency–Load Interaction in the Pre– and Postbuckling Ranges

PVP-Vol. 225/NE-Vol. 7, Recent Advances in
Structural Mechanics
ASME 1991

EFFECTS OF SHEAR DEFORMATION AND ROTARY INERTIA ON THE PULSE BUCKLING OF IMPERFECT PLATES

Judah Ari-Gur
Department of Mechanical Engineering
Western Michigan University
Kalamazoo, Michigan

Isaac Elishakoff
Department of Mechanical Engineering
Florida Atlantic University
Boca Raton, Florida

ABSTRACT

The dynamic buckling of geometrically imperfect rectangular plates under longitudinal inplane compressive pulse is studied. The transverse shear and rotary inertia terms are included in the analysis and their effects are investigated for various pulse frequencies and initial imperfections. A collapse-type dynamic buckling criterion is defined and buckling results are obtained. The dynamic buckling values are compared to those for shear-rigid plates. The results show that the classical plate theory overestimates the resistance of plates to dynamic pulse buckling.

INTRODUCTION

The buckling of rectangular plates under dynamic in-plane compression was studied for constant rate of loading, as in a rigid universal testing machine, by Birkgan and Vol'mir (1961) and Ekstrom (1973). Later, Ari-Gur et al (1981, 1985) investigated the dynamic buckling under collision impact loading. Their studies, both experimental and theoretical, were limited to low velocity impact, where incipient buckling occurs within the range of elastic behavior of the material. Recently, the elastic pulse buckling of anisotropic composite plates was studied by Ari-Gur (1989, 1991). The plastic collapse of plates due to high intensity impulsive loads has been reviewed in the monograph by Lindberg and Florence (1987). With a few exceptions, it has been observed that, for short duration pulses, the buckling loads are higher than the static ones, but the ratios of dynamic to static buckling loads are much smaller than those obtained for columns. Also, the dynamic buckling loads are sensitive to initial geometrical imperfections. In general, short pulse durations and small imperfections result in higher dynamic buckling loads.

To the best of our knowledge, the effects of transverse shear deformations have not been included in the existing published theoretical studies of the dynamic pulse buckling of plates. There are indications, however, that these complicating effects may be significant. A recent study, by Ari-Gur and Elishakoff (1990), of the dynamic pulse buckling of columns, demonstrated an appreciable effect of transverse shear deformations on the buckling resistance of the studied structures. The objective of the present paper is, therefore, to study the influence of transverse shear deformations and rotary inertia on the dynamic pulse buckling of plates, in comparison with results obtained through the classical plate theory.

ANALYSIS

Consider a rectangular plate of a length a, width b and thickness h, subjected to a compression pulse in the longitudinal direction x (Figure 1). The plate has an initial geometrical imperfection $w_o(x,y)$. Due to the pulse, transient deformations occur and time-dependent in-plane displacements u(x,y,t) and v(x,y,t), lateral deflections w(x,y,t) and shear angles $\gamma_x(x,y,t)$ and $\gamma_y(x,y,t)$ are generated.

Differential Equations

A first-order shear deformation theory (FST), as proposed by Mindlin (1951), is adopted here. Assuming that a line perpendicular to the neutral surface of the undeformed plate remains straight (but not necessarily normal) throughout the response, and assuming small rotations of the cross-section and neutral surface, the differential equations of dynamic equilibrium of the Mindlin-type plate are:

$$I_1 \ddot{u} = N_{x,x} + N_{xy,y} - [Q_x (w_{,x} - \gamma_x)]_{,x} \qquad (1)$$

$$I_1 \ddot{v} = N_{y,y} + N_{xy,x} - [Q_y (w_{,y} - \gamma_y)]_{,y} \qquad (2)$$

$$I_1 \ddot{w} = [Q_x + N_x (w_{,x} - \gamma_x) + N_{xy} w_{,y}]_{,x} + [Q_y + N_y (w_{,y} - \gamma_y) + N_{xy} w_{,x}]_{,y} \qquad (3)$$

$$I_2 (\ddot{w}_{,x} - \ddot{\gamma}_x) = Q_x + M_{x,x} + M_{xy,y} - N_x \gamma_x \qquad (4)$$

$$I_2 (\ddot{w}_{,y} - \ddot{\gamma}_y) = Q_y + M_{y,y} + M_{xy,x} - N_y \gamma_y \qquad (5)$$

where $f_{,x} = \partial f/\partial x$, $\dot{f} = \partial f/\partial t$ and, as shown in Figure 2, N_x and N_y are the inplane normal forces, N_{xy} is the inplane shear force, M_x and M_y are the bending moments, M_{xy} is the warping moment and Q_x and Q_y are the transverse shear forces, all of them per unit length of the plate cross-section. The angles γ_x and γ_y are the transverse shear strains or the rotations of the cross-section due to shear only, whereas $\gamma_i - (w - w_o)_{,i}$ (i=x,y) is the total rotation of the cross-section. Note that w is the total distance from the x-y plane, hence the actual lateral deflection is $w - w_o$. I_1 and I_2 are the translational and

rotational inertia terms, respectively. For uniform density plates, they are:

$$I_1 = \rho h \tag{6}$$

$$I_2 = \frac{1}{12}\rho h^3 \tag{7}$$

Note that the present theory includes the inplane forces and inertia terms that were not included by Mindlin (1951), whose paper dealt with lateral vibrations only. When the inplane forces (N_{ij}) and inertia terms ($I_1\ddot{u}$, $I_1\ddot{v}$) are neglected, Equations (1) and (2) vanish and Equations (3)-(5) are reduced to the corresponding Mindlin theory equations.

Also, for $\gamma_x=\gamma_y=0$, substitution of the shear forces Q_x and Q_y from Equations (4)-(5) into Equation (3), reduces the equations to the classical plate theory (CPT), as in the paper by Ari-Gur et al (1981).

The forces and moments relate to the deformations through the following equations:

$$N_x = \frac{Eh}{1-\nu^2}(\varepsilon_x+\nu\varepsilon_y) \tag{8}$$

$$N_y = \frac{Eh}{1-\nu^2}(\varepsilon_y+\nu\varepsilon_x) \tag{9}$$

$$N_{xy} = Gh\gamma_{xy} \tag{10}$$

$$M_x = D(\kappa_x+\nu\kappa_y) \tag{11}$$

$$M_y = D(\kappa_y+\nu\kappa_x) \tag{12}$$

$$M_{xy} = (1-\nu)D\kappa_{xy} \tag{13}$$

$$[Q_x\ ;\ Q_y] = kGh[\gamma_x\ ;\ \gamma_y] \tag{14}$$

where E is the modulus of elasticity, ν the Poisson's ratio, G the shear modulus, k the shear shape factor, h the plate thickness and D the bending stiffness:

$$D = \frac{Eh^3}{12(1-\nu^2)} \tag{15}$$

The strain-displacement relations are:

$$\varepsilon_{ij} = \frac{1}{2}(u_{i,j}+u_{j,i}) + \frac{1}{2}(w_{,i}w_{,j}-w_{0,i}w_{0,j}) \quad ; \quad i,j=x,y \tag{16}$$

where $\varepsilon_{xx}=\varepsilon_x$, $\varepsilon_{yy}=\varepsilon_y$, $u_x=u$, $u_y=v$ and $\gamma_{xy}=2\varepsilon_{xy}$. The curvatures are:

$$\kappa_{ij} = (w-w_0)_{,ij} - \frac{1}{2}(\gamma_{i,j}+\gamma_{j,i}) \quad ; \quad i,j=x,y \tag{17}$$

The differential equations (1)-(5) should be integrated to solve for the response functions u, v, w, γ_x and γ_y. Differentiating Equation (3) in respect to x and then substituting $\ddot{w}_{,x}$ in Equation (4), and similarly for $\ddot{w}_{,y}$ in Equation (5), provide five decoupled differential equations for $\ddot{u}$, $\ddot{v}$, $\ddot{w}$, $\ddot{\gamma}_x$ and $\ddot{\gamma}_y$. The decoupled equations will be presented later in a nondimensional formulation.

Boundary and Initial Conditions

In order to solve the system of differential equations, four boundary conditions are required along each edge -- two lateral and two inplane conditions. The present study assumes that the edges are simply-supported:

$$\begin{aligned} w &= 0 \ ; \ M_x = 0 \quad at \quad x=0\ ,\ a \\ w &= 0 \ ; \ M_y = 0 \quad at \quad y=0\ ,\ b \end{aligned} \tag{18}$$

and frictionless:

$$N_{xy} = 0 \quad at \quad x=0,a \quad y=0,b \tag{19}$$

It is also assumed that the edges remain straight throughout the deformation and their normal displacements are restrained:

$$\begin{aligned} u &= 0 \quad at \quad x=a \\ u_{,y} &= 0 \quad at \quad x=0 \\ v &= 0 \quad at \quad y=0,b \end{aligned} \tag{20}$$

The uniform longitudinal displacement of the loaded edge is dictated by the load:

$$N_x = -N_0(t) \quad at \quad x=0 \tag{21}$$

The plate is assumed to be at rest before the load is applied. Hence, the initial conditions at t=0 read:

$$\begin{aligned} u{=}0 &\ , \ \dot{u}{=}0 \\ v{=}0 &\ , \ \dot{v}{=}0 \\ w{=}w_o &\ , \ \dot{w}{=}0 \\ \gamma_x{=}0 &\ , \ \dot{\gamma}_x{=}0 \\ \gamma_y{=}0 &\ , \ \dot{\gamma}_y{=}0 \end{aligned} \tag{22}$$

The shape of the initial geometrical imperfection $w_o(x,y)$ is not restricted. However, the results for the present study were obtained for

$$w_o(x) = W_o \sin\frac{\pi x}{a}\sin\frac{\pi y}{b} \tag{23}$$

which kinematically agrees with the assumed simply-supported boundary conditions.

Nondimensional Formulation

For better understanding and illustration of the significant variables of the problem, a nondimensional formulation was developed and will be employed in the presentation of the results and the discussion. We define the nondimensional response functions:

$$\bar{u} = \frac{u}{a} \ , \ \bar{v} = \frac{v}{b} \ , \ \bar{w} = \frac{w}{h} \tag{24}$$

coordinates:

$$\xi = \frac{x}{a} \ , \ \eta = \frac{y}{b} \ , \ \tau = \frac{t}{a}\sqrt{\frac{E}{(1-\nu^2)\rho}} \tag{25}$$

and parameters:

$$\bar{a} = \frac{a}{b} \ , \ \lambda = \frac{b}{h} \ , \ \varepsilon_0(\tau) = N_0(t)\frac{1-\nu^2}{Eh} \tag{26}$$

Note that the nondimensional time τ=1 corresponds to the time for the propagation of a longitudinal wave along the length (a) of the plate. Also, for isotropic materials, $\bar{D}$=1 and G=E/2(1+ν). The differential equations then become:

$$\ddot{\bar{u}} = \varepsilon_{\xi,\xi} + \nu\varepsilon_{\eta,\xi} + \frac{1-\nu}{2}\left\{\bar{a}\gamma_{\xi\eta,\eta} - k\left[\gamma_\xi\left(\frac{1}{\lambda\bar{a}}\bar{w}_{,\xi} - \gamma_\xi\right)\right]_{,\xi}\right\} \quad (27)$$

$$\ddot{\bar{v}} = (\bar{a})^2(\varepsilon_{\eta,\eta} + \nu\varepsilon_{\xi,\eta}) + \frac{1-\nu}{2}\left\{\bar{a}\gamma_{\xi\eta,\xi} - k(\bar{a})^2\left[\gamma_\eta\left(\frac{1}{\lambda}\bar{w}_{,\eta} - \gamma_\eta\right)\right]_{,\eta}\right\} \quad (28)$$

$$\ddot{\bar{w}} = [(\varepsilon_\xi + \nu\varepsilon_\eta)(\bar{w}_{,\xi} - \lambda\bar{a}\gamma_\xi)]_{,\xi} + (\bar{a})^2[(\varepsilon_\eta + \nu\varepsilon_\xi)(\bar{w}_{,\eta} - \lambda\gamma_\eta)]_{,\eta} + \bar{a}\frac{1-\nu}{2}\left[k\lambda(\gamma_{\xi,\xi} + \bar{a}\gamma_{\eta,\eta}) + (\gamma_{\xi\eta}\bar{w}_{,\eta})_{,\xi} + (\gamma_{\xi\eta}\bar{w}_{,\xi})_{,\eta}\right] \quad (29)$$

$$\ddot{\gamma}_\xi = \frac{1}{\bar{a}\lambda}\bar{w}_{,\xi\tau\tau} - 12(\bar{a}\lambda)^2\left(k\frac{1-\nu}{2} - \varepsilon_\xi - \nu\varepsilon_\eta\right)\gamma_\xi + -\bar{a}\lambda\left[(\kappa_\xi + \nu\kappa_\eta)_{,\xi} + \bar{a}(1-\nu)\kappa_{\xi\eta,\eta}\right] \quad (30)$$

$$\ddot{\gamma}_\eta = \frac{1}{\lambda}\bar{w}_{,\eta\tau\tau} - 12(\bar{a}\lambda)^2\left(k\frac{1-\nu}{2} - \varepsilon_\eta - \nu\varepsilon_\xi\right)\gamma_\eta + -\bar{a}\lambda\left[\bar{a}(\kappa_\eta + \nu\kappa_\xi)_{,\eta} + (1-\nu)\kappa_{\xi\eta,\xi}\right] \quad (31)$$

where the nondimensional curvatures are the flexural strains obtained by multiplying the dimensional curvatures of Equation (17) by the thickness h, for example : $\kappa_{\xi\eta}=\kappa_{xy}h$.

Numerical Approach

The finite-difference-method (FDM) was employed to solve the problem, with the differential equations approximated over the finite time interval $\Delta\tau$ and plate element $\Delta\xi$ by $\Delta\eta$. In order to allow for finite $\Delta\xi$ and $\Delta\eta$, which are not necessarily negligible relative to the thickness, coefficients α_x and α_y, defined as:

$$\alpha_x = 1 + \left(\frac{\Delta x}{h}\right)^2 = 1 + (\Delta\xi\,\bar{a}\lambda)^2$$
$$\alpha_y = 1 + \left(\frac{\Delta y}{h}\right)^2 = 1 + (\Delta\eta\,\lambda)^2 \quad (32)$$

were incorporated into Equations (4)-(5), which then read:

$$I_2(\alpha_x\ddot{w}_{,x} - \ddot{\gamma}_x) = Q_x + M_{x,x} + M_{xy,y} - N_x\gamma_x \quad (33)$$

$$I_2(\alpha_y\ddot{w}_{,y} - \ddot{\gamma}_y) = Q_y + M_{y,y} + M_{xy,x} - N_y\gamma_y \quad (34)$$

α_x and α_y do not appear in the differential equations (4)-(5) since $\alpha_x=1$ for $\Delta x \ll h$ and $\alpha_y=1$ for $\Delta y \ll h$. However, the additional terms, which represent the rotational inertia due to the finite lengths of the plate element, are needed for use in the numerical solution, where Δx and Δy have discrete values that may be significant. For example, if $\Delta x=a/20$ is chosen for a plate with a/h=40, then $\alpha_x=5$ is obtained, and using $\alpha_x=1$ will cause a large numerical error.

The incorporation of α_x and α_y do not affect Equations (27)-(29), but Equations (30)-(31) become:

$$\ddot{\gamma}_\xi = \frac{\alpha_x}{\bar{a}\lambda}\bar{w}_{,\xi\tau\tau} - 12(\bar{a}\lambda)^2\left(k\frac{1-\nu}{2} - \varepsilon_\xi - \nu\varepsilon_\eta\right)\gamma_\xi + -\bar{a}\lambda\left[(\kappa_\xi + \nu\kappa_\eta)_{,\xi} + \bar{a}(1-\nu)\kappa_{\xi\eta,\eta}\right] \quad (35)$$

$$\ddot{\gamma}_\eta = \frac{\alpha_y}{\lambda}\bar{w}_{,\eta\tau\tau} - 12(\bar{a}\lambda)^2\left(k\frac{1-\nu}{2} - \varepsilon_\eta - \nu\varepsilon_\xi\right)\gamma_\eta + -\bar{a}\lambda\left[\bar{a}(\kappa_\eta + \nu\kappa_\xi)_{,\eta} + (1-\nu)\kappa_{\xi\eta,\xi}\right] \quad (36)$$

Using the central difference approximation for the time derivatives in Equations (27)-(29) and (35)-(36), explicit equations for u, v, w, γ_ξ and γ_η at the time $\tau+\Delta\tau$ are obtained. The differential equations are then integrated through time-stepping.

The central difference approximation was employed also for the spatial derivatives, except for the boundaries, where forward schemes were used at $\xi=0$ and $\eta=0$, and backward schemes at $\xi=1$ and $\eta=1$. All the results presented at this paper were obtained for $\Delta\xi=\Delta\eta\le0.1$ and $\Delta\tau\le\Delta\xi$.

RESULTS AND DISCUSSION

The time-dependent load $\epsilon_o(\tau)$ in the analysis is not restricted to a certain time-history. Since a half-sine pulse shape can be varied in intensity (ϵ_o) and duration (T), it was chosen for the present analysis. The applied pulse is then:

$$\varepsilon_o(\tau) = \begin{cases} \varepsilon_o \sin\left(\dfrac{\pi\tau}{T}\right) & , \quad 0\le\tau\le T \\ 0 & , \quad \tau\ge T \end{cases} \quad (37)$$

Buckling Criterion

A buckling criterion that relates the peak axial displacement ($\bar{u}$) to the peak force (ϵ_o) at the loaded edge ($\xi=0$) of the plate is employed in the present study. Buckling is defined when a small increase in the pulse intensity causes a sharp increase of the end displacement (Figure 3). The meaning of this is that at a certain level of load intensity the longitudinal resistance of the plate is substantially diminished and a slightly stronger pulse causes a structural collapse. This criterion resembles the Budiansky-Hutchinson (1964) dynamic buckling criterion (see also Hutchinson and Budiansky (1966)), for which buckling occurs when a small increase in the load intensity causes a transition from a bounded response to an unbounded one.

Shear Effects

The effects of the transverse shear deformations are studied here by comparing results obtained through the present first-order shear theory (FST) with those for the classical plate theory (CPT). The shear shape factor for isotropic plates is k=5/6=0.83, whereas the rigid transverse shear assumption of the classical theory is equivalent to $k\to\infty$.

Results for $\bar{a}$=1, λ=50, ν=0.3 and $\bar{w}_0$=0.01 are presented in Figures 4 (a) and (b). The nondimensional half-period of the fundamental natural frequency of this plate is $T_b/2=27.6$. For a relatively short pulse duration of T=10, the classical plate theory overestimates the FST buckling load by more than a factor of two, as shown in Figure 4(a). Moreover, for a longer pulse duration of T=50, see Figure 4(b), the CPT buckling load is almost four times larger than the shear theory prediction. These ratios, however, are lower than those obtained by Ari-Gur and Elishakoff (1990) for columns of similar length-to-thickness ratio.

Note also that the FST buckling load for T=50 is lower than the linear static buckling load. This means that neglecting shear effects and, as acceptable in common practice, assuming that the dynamic buckling load is higher than the static one, may lead to dangerous predictions.

Effects of Pulse Duration

The dynamic buckling loads under short duration pulses are significantly higher than those for quasi-static loads. This general prediction is independent of the theory employed. However, there are differences between both theories in the relative proportions. Figure

5(a) presents the FST results for impulsive (T=10), dynamic (T=25) and quasi-static (T=50) loads. The impulsive buckling load is more than four times larger than the dynamic and nine times larger than the quasi-static buckling loads. A comparison with Figure 5(b) for classical theory shows smaller ratios of two and five, respectively. Since the difference between the present FST and CPT formulations is not only in the inclusion of transverse shear deformations but also rotary inertia terms, it is possible that the relatively large stiffening for T=10 in Figure 5(a) is due to the added contribution of rotary inertia resistance.

Imperfection Effects

Dynamic pulse buckling loads are sensitive to initial geometrical imperfections. A comparison between W_0=0.01 and W_0=0.1 is presented in Figure 6. It appears that the relative difference in buckling loads between the two imperfection values is smaller for the FST results than those for the CPT results. Hence, when the shear deformation theory is employed, the imperfection sensitivity is smaller and the significance of exact imperfection characterization appears to decrease.

Effects of Thickness

The effects of transverse shear and rotary inertia are more pronounced for thick plates. The results in Figures 4-6 are for b/h=50 for which, as was shown in Figure 4(a), the impulsive buckling load predicted by the first-order shear theory (FST) is less than half of that predicted by the classical plate theory (CPT). The difference is much smaller for thinner plates. Results for b/h=100 are presented in Figure 7, and for this thinner plate the FST buckling load is only about 25% less than the CPT prediction.

CONCLUDING REMARKS

The effects of transverse shear deformation on the dynamic pulse buckling of isotropic plates were studied. It was shown, for simply-supported plates, that the dynamic buckling loads obtained through a Mindlin-type first-order transverse shear deformation theory are lower than those predicted through the classical plate theory. Dynamic buckling results obtained through the classical theory, which neglects the transverse shear effects, may be significantly overestimated (factors of up to four were obtained here) relative to those obtained from a theory that includes shear effects.

REFERENCES

Ari-Gur, J., 1989, "Dynamic Pulse Buckling of Angle-Ply Composite Plates", in: *Recent Advances in Impact Dynamics of Engineering Structures*, D. Hui and N. Jones, eds., AMD-Vol. 105 and AD-Vol. 17, ASME, pp. 121-127.

Ari-Gur, J., 1991, "Dynamic Buckling of Composite Plates", *Proc. of the Fifth ANSYS Int. Conf.*, Pittsburgh, pp. 20.28-20.38.

Ari-Gur, J. and Elishakoff, I., 1990, "Effects of Shear Deformation and Rotary Inertia on the Dynamic Pulse Buckling of a Structure", in: *Impact and Buckling of Structures*, D. Hui and I. Elishakoff, eds., AD-Vol. 20 and AMD-Vol. 114, ASME, pp. 71-75.

Ari-Gur, J., Singer, J. and Weller, T., 1981, "Dynamic Buckling of Plates Under Longitudinal Impact", Israel Journal of Technology, Vol. 19, No. 1, 57-64.

Ari-Gur, J. and Weller, T., 1985, "Experimental Studies with Metal Plates Subjected to Inplane Axial Impact", TAE No. 580, Department of Aeronautical Engineering, Technion, Haifa, Israel.

Birkgan, A.Y. and Vol'mir, A.S., 1961, "An Investigation of the Dynamic Stability of Plates Using an Electronic Digital Computer", *Sov. Phys. Dokl.*, Vol. 5, No. 6, pp. 1364-1366.

Budiansky, B. and Hutchinson, J.W., 1964, "Dynamic Buckling of Imperfection Sensitive Structures", *Proc. of the Eleventh Int. Congress of Applied Mechanics*, Munich, Springer-Verlag, 1966, pp. 636-651.

Ekstrom, R.E., 1973, "Dynamic Buckling of a Rectangular Orthotropic Plate", *AIAA J.*, Vol. 11, No. 12, pp. 1655-1659.

Hutchinson, J.W. and Budiansky, B., 1966, "Dynamic Buckling Estimates", *AIAA Journal*, Vol. 4, No. 3, pp. 525-530.

Lindberg, H.E. and Florence, A.L., 1987, *Dynamic Pulse Buckling*, Martinus Nijhoff Publ., Dordrecht, Ch. 2.

Mindlin, R.D., 1951, "Influence of Rotatory Inertia and Shear on Flexural Motions of Isotropic, Elastic Plates", Journal of Applied Mechanics, Trans. ASME, Vol. 73, No.1, 31-38.

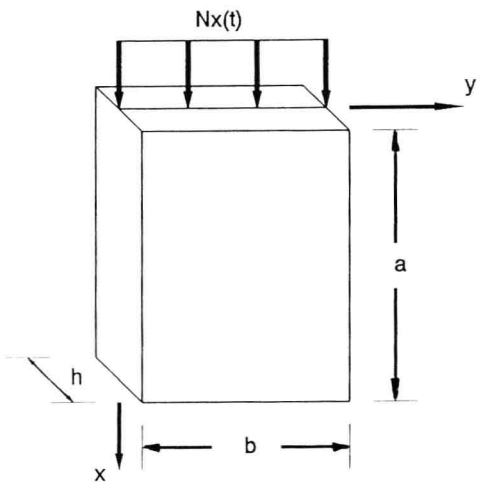

Fig. 1 THE PLATE

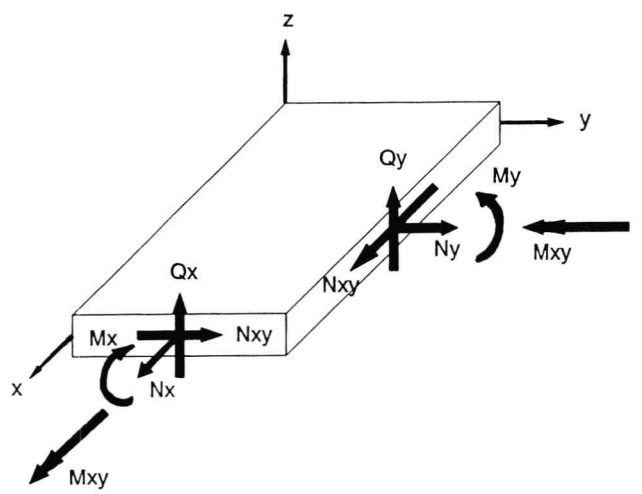

Fig. 2 ELEMENT POSITIVE FORCES AND MOMENTS

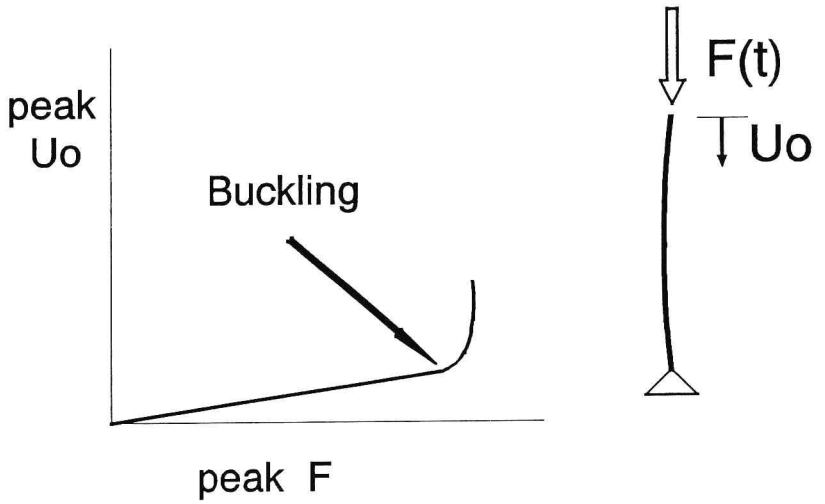

Fig. 3 COLLAPSE-TYPE BUCKLING CRITERION

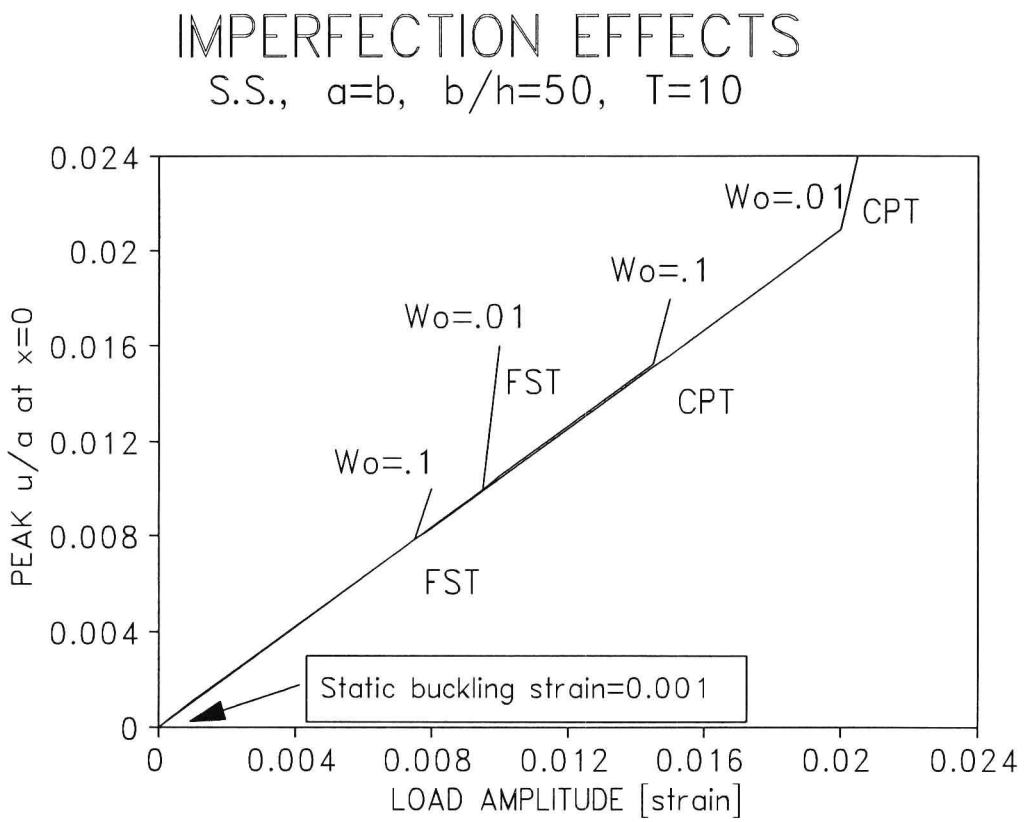

Fig. 6 EFFECTS OF INITIAL IMPERFECTION

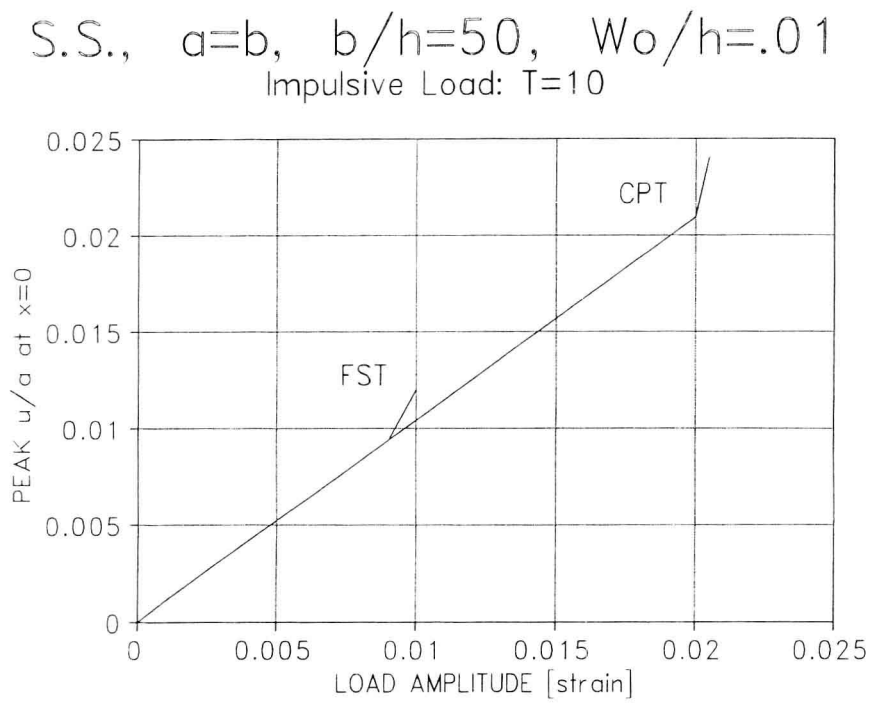

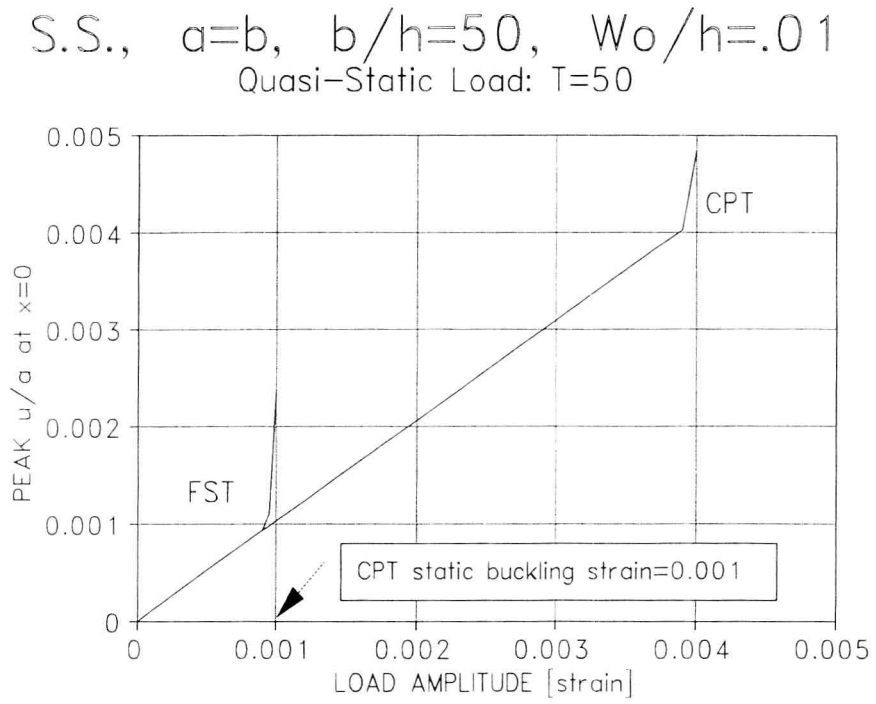

Fig. 4 EFFECTS OF TRANSVERSE SHEAR DEFORMATIONS
(a) Impulsive Load
(b) Quasi-Static Pulse

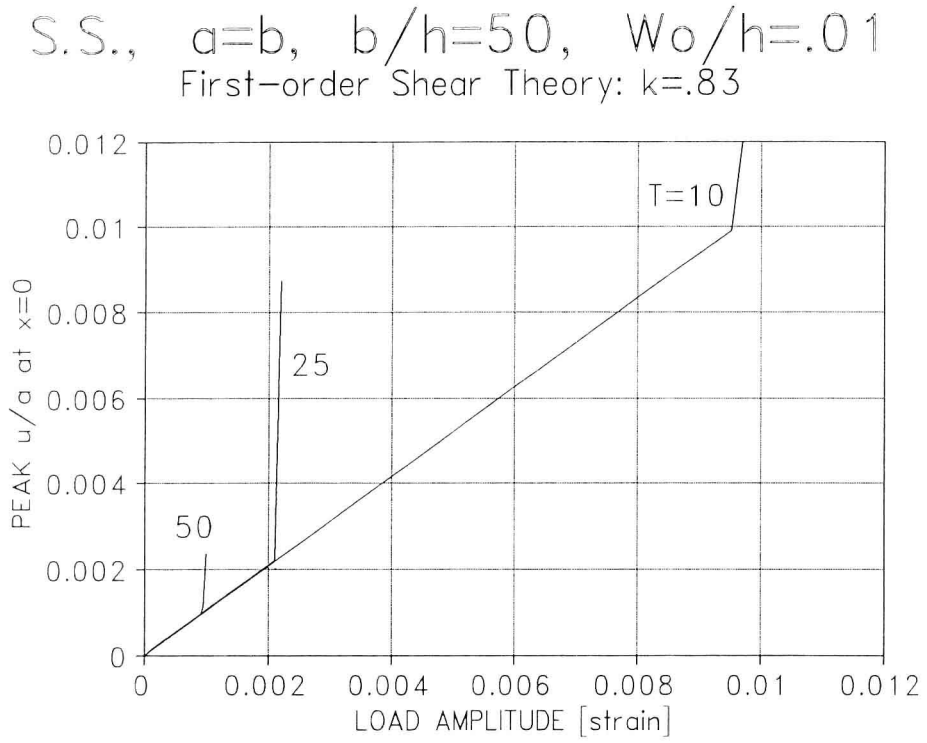

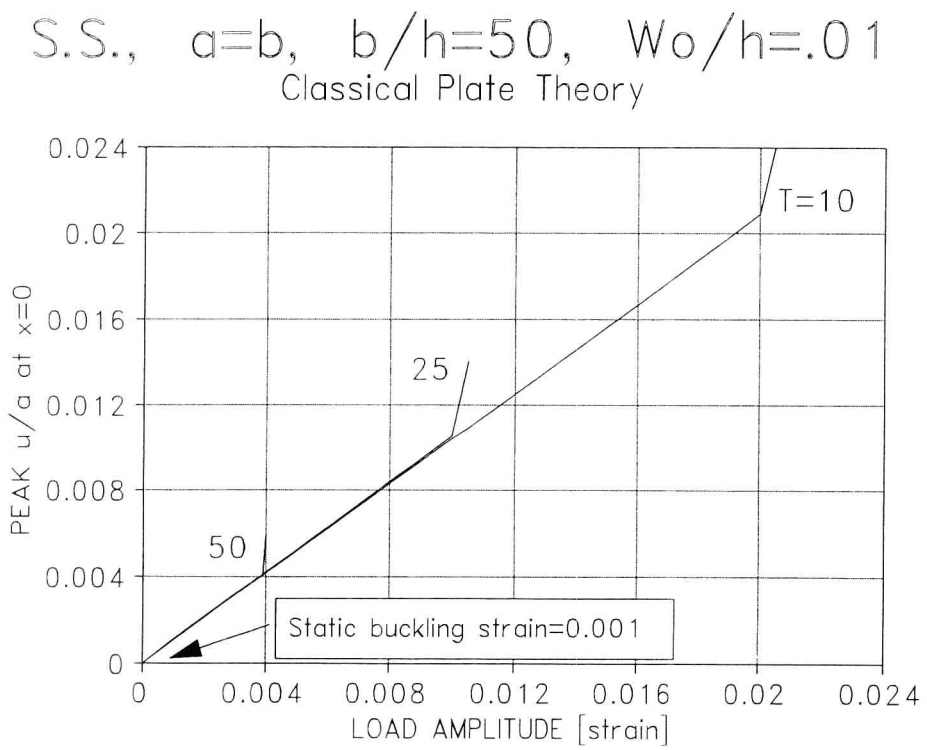

Fig. 5 EFFECTS OF PULSE DURATION
(a) First-order Shear-deformation Theory
(b) Classical Plate Theory